Journal of Mathematics in Industry
a SpringerOpen Journal

RESEARCH Open Access

Pricing of insurance-linked securities: a multi-peril approach

Krzysztof Burnecki[1*], Marek A. Teuerle[1] and Martyna Zdeb[1]

*Correspondence:
krzysztof.burnecki@pwr.edu.pl
[1]Faculty of Pure and Applied Mathematics, Hugo Steinhaus Center, Wroclaw University of Science and Technology, Wyspianskiego 27, 50-370 Wroclaw, Poland

Abstract

In this paper we build a methodology for pricing of insurance-linked securities which are tied to multiple natural catastrophe perils. As a representative example, we construct a multi-peril catastrophe (CAT) bond which can be linked to the industry loss indices or actual losses incurred by an insurer. We provide pricing formulas for such CAT bonds. We illustrate the introduced methodology on the US natural catastrophe data obtained from Property Claim Services (PCS). Within this dataset, we specifically examine two types of risks: losses associated with wind and thunderstorm events, and those linked to winter storm events. Then, we fit and validate the underlying compound non-homogeneous Poisson processes taking into account the fact that the data are left-truncated. The best fitted loss distributions appear to be Burr and Generalised Extreme Value and for the first peril and log-normal for the second. Finally, we visualise the zero-coupon CAT bond prices for the selected best-fitted models.

Keywords: Insurance-linked security; Catastrophe bond; Arbitrage-free price; Multiple perils; Risk management

1 Introduction

Insured losses have been elevated over the last five years due to recurring high-loss secondary peril events such as severe convective storms, floods and wildfires. Coming after a dip in 2012–2016, the higher insured losses of 2017–2021 signal a return to a long-term growth trend of 5–7%. Insurance covered USD 119 billion of 2021 economic losses, the fourth highest on record, of which USD 111 billion was compensation for damage resulting from natural catastrophes [51].

To date, the majority of losses resulting from natural catastrophes have been due to the increasing accumulation of insured exposure (from human and physical assets) that has arisen with economic growth and urbanisation. In the coming decades, climate change will be one of the many factors that will contribute markedly to the increase in economic and, as a consequence, insured losses. In particular, as world temperatures rise, and humans continue to expand mankind's urban footprints, the frequency and severity of losses resulting from severe natural catastrophe events will increase [50].

Discussions with practitioners, especially those in the global reinsurance industry, have consistently highlighted that the top region-perils impacting yearly insured losses are: US

earthquakes, US hurricanes, EU windstorms, EU floods and US convective storms. Dire warnings about devastating hurricanes were a hot topic at the COP21 climate talks in Paris.

Up to 2013, US convective storm has accounted for, on average, one-third of average annual losses [46]. However, US earthquake and US hurricane perils remain the top contributors. Each year, Swiss Re publishes a list of the 40 most costly industry insured natural-catastrophe related losses - apart from the Japanese earthquake and tsunami of 2011, the most notable largest losses have comprised three US hurricanes (i.e. Katrina in 2005, Sandy in 2012 and Andrew in 1992) and a US earthquake (the Northridge earthquake of 1992). It is important to bear in mind that these losses impacted not only a single US state, but multiple ones instead [50].

Windstorms are the peak weather-related natural catastrophe risk in Europe. There has been a lull in large-scale storm disasters in recent years, but the 1999 storm series of Lothar and Martin, and the North Sea storm surge in 1953, remain significant tail risk events. The risk is dominated by strong natural variability: the history of European windstorms shows a strong multi-decadal pattern.

Flood risk in Europe has changed in the last 50 years. Climate change and urbanisation make the flood risk landscape dynamic. Flood is another peak risk in Europe. The central European floods of 2002 and 2013 serve as important reminders of the loss potential of this peril. Natural variability is an important aspect, but studies also confirm that a changing climate has had a notable impact on the seasonality as well as on the severity and frequency of flood events in Europe, with clear regional patterns being noted [50]. A 2019 systematic analysis of a comprehensive dataset of flood observations detected both increasing and decreasing trends, by region, over the last five decades [5]. According to this study, large parts of central and north western Europe experienced an increase of up to 11% per decade in annual river-flood discharge, while the Mediterranean area and eastern Europe showed significant decreases. Flood severity depends not only on precipitation levels and the extent of surface sealing but also on soil moisture, snow-melt and the occurrence of persistent weather patterns, all of which are influenced by warming temperatures. Moreover, a flood risk management paper by [40] with an analysis of global data that spans over the last 100 years shows the heavy-tailed characteristic of flood losses.

There is a need to dynamically track the effects of a warming climate, adapting models to an ever-evolving risk landscape. New understandings into risk assessment need to be embedded, and novel ways of risk transfer (accessible to larger pools of investors) need to be continually considered and developed.

Against this backdrop, it is clear that there is a greater need for novel risk management instruments in the economic and financial system, with the view that these instruments will further benefit the social and political systems as well. In this regard, insurance-linked securities (ILS) solutions have been at the fore. ILS are investment assets linked to insurance-related, non-financial risks such as natural disasters, life and health insurance risks including mortality or longevity. To date, most ILS issues have been collateralized reinsurance and catastrophe bonds (CAT bonds).

In view of the discussion above, we present the structure of this paper. In Sect. 2 we present pricing approaches for ILS with a special emphasis on pricing catastrophe (CAT) bonds. In Sect. 3 we introduce a multi-peril CAT bond model. Here we consider two payoff structures for CAT bonds, namely the zero-coupon (ZC) and coupon-paying (CP). For

the analysed CAT bonds, we provide pricing formulas. In Sect. 4 we fit the model to wind and thunderstorm, and winter storm natural catastrophe data obtained from PCS. The analysis incorporates the calibration and validation of statistical processes within the two-peril framework by taking into account the left-truncated nature of the data. Finally, we illustrate the calculated prices of a two-peril ZC CAT bond for the best fitted models. Section 5 summarises the main findings of the paper.

2 Insurance-linked securities. Literature review

ILS are an innovative way to increase insurance capacity. They are a means of ceding insurance-related risks to the capital markets. ILS are collateralized to eliminate credit risk for investors. Investors benefit from a low correlation with other asset classes and higher interest rates than for government bonds. There is no counterparty risk as with traditional reinsurance. Funds are held in a safe, bankruptcy-remote Special Purpose Vehicle (SPV). An SPV has two functions; it provides reinsurance for insurance companies and issues securities to investors.

The most prominent type of such products are catastrophe bonds (CAT) [1] so they will be of our primary interest. If there is no catastrophic event, or trigger event, before the maturity date of the contract, investors receive back their principal investment at maturity on top of the interest payments they have received. If a catastrophic event occurs, investors may sacrifice their principal and interest.

The creation of CAT bonds, along with allied financial products such as catastrophe insurance options, was motivated in part by the need to cover the massive property insurance industry payouts of the early- to mid-1990s. They also represent a 'new asset class' in that they provide a mechanism for hedging against natural disasters, a risk that is essentially uncorrelated with the capital market indices [21]. Subsequent to the development of the CAT bond, the class of referenced disasters has grown considerably.

The record pace of issuance in 2021 continued during the third quarter, as 25 tranches of notes combined brought more than USD 2.7 billion of new risk capital to the market, beating the prior year period by more than USD 1 billion. 2021 is the first time Q3 issuance has exceeded USD 2.5 billion [1].

CAT bonds have been loosely classified into three main types: indemnity-linked (involves the actual losses of the bond-issuing insurer), index-linked (involves, in the US, for example, an index created from PCS loss estimates) and parametric (is based on, for example, the Richter scale readings of the magnitude of an earthquake at specified data stations), see [19]. Such a classification is based on the 'trigger' of the bond, that is the event (or set or even sequence thereof) that causes the bond to release the capital to the issuer. In this paper, we focus on index-linked and indemnity CAT bonds, which have the largest outstanding issuance in the CAT bond market [1].

Most CAT bonds are based on a single trigger. However, in some cases, multiple triggers are used. CAT bonds are often divided into two tranches that exhibit different risk-return profiles or vary in terms of trigger, reference peril, and covered territory. An average maturity of traded CAT bonds is three years. Outstanding market volume is almost evenly split between per-occurrence and annual-aggregate CAT bonds.

Most of the research devoted to the modelling of natural catastrophes and then pricing the respective risk securitization solution deals with the problem of arbitrage-free valuation and the aspects of completeness of the market. The first works that addressed the

problem of pricing included relatively simple models [16, 23]. The literature was then further developed by including stochastic interest rate scenarios in both discrete and continuous-time frameworks, as well as the contingent claim approach [12, 27, 37, 41, 42, 53]. Recently, we have also observed an increasing interest in developing and pricing more sophisticated financial instruments, such as catastrophe options, catastrophe futures, contingent convertible catastrophic bonds, and catastrophe risk swaps [7, 10, 38].

In practice, issuance of a catastrophe bond typically requires the engagement of a specialised modelling firm to quantify the catastrophe risk. The risk modeller estimates the probability of first loss (PFL) and provides an estimate of the expected loss (EL) for investors. The risk modelling companies include AIR Worldwide (Verisk), Risk Management Solutions (RMS) and EQECAT (CoreLogic).

The relationship between price spreads and EL has been studied by several authors. [33] analysed a simple model, where the spread was a function of EL, PFL and conditional expected loss. The regression approach with a single explanatory variable being EL was investigated by [32]. Twenty years of data (2001-2020), 757 individual ILS were used to fit the model, resulting in $R^2 = 0.58$. The regression approach with different explanatory variables related to the financial environment, the CAT market, and other factors was studied by [8]. The analysis covered the period from 1997 to the end of 2012 and uses a data set, compiled from many sources, that contained 466 tranches issued to the primary market during that period. The adjusted R^2 for this model was 0.89. We finally note on the works on implied Poisson intensities from regularly observed prices [4], machine learning approach investigated by [26, 31], Fréchet–Wasserstein mean utility functionals found useful for designing and pricing a CAT bond [43], and pricing the catastrophe bonds on earthquake risk with the help of extreme value theory [55].

It is also noticed that some of the existing literature already raised the problem of multi-peril ILS, see for example the pioneering work by Lane [34], where the author explored "arbitrage-equivalent" pricing in which covers can be either bought or sold. In [44] the author addresses pricing of an insurance-linked security that derived its value based on two underlying processes: catastrophic insured property losses and catastrophic mortality. In [29], based on seismic zones, the Italian territory was divided into three zones and three CAT bonds with different levels of default risk were priced. Furthermore, in [47] an empirical study of California earthquake data within the multi-peril risk model was conducted. Very recently, in [52], the authors analysed a three-event rainstorm CAT bond based on the resulting losses due to rainstorms in China during 2006–2020.

3 Multi-peril CAT bonds

In this part, we first present the pricing framework for a single-peril CAT bond and then construct a multi-peril CAT bond for which we build a pricing methodology. The ultimate goal is to present general pricing formulas for the ZC CAT bonds and CP CAT bonds in single- and multi-peril frameworks.

For both single- and multi-peril cases, we assume that the trigger of respective CAT bonds is index-linked or is related to actual losses of an insurer, which is in line with many of the CAT bonds (see, for instance, [17, 28, 37] and [24]). One of the most commonly issued index-linked CAT bonds is the bond that is tied to the PCS industry index. The bond is triggered, for most of such CAT bonds, if the PCS index representing the aggregate natural catastrophe losses exceeds some contractually-specified threshold level.

The general pricing technique in this work is based on the incomplete market framework of [39]. This is a typical approach to pricing of financial products with payoff dependent on natural disaster events; see, for example, [3, 30, 35–37, 41, 53] and [13]. The key to effective pricing is based on the following assumption.

Assumption 1 Investors are risk-neutral towards the jump risk posed by the natural catastrophe-risk variables.

Assumption 1 can be understood as a statement that natural catastrophes are treated as idiosyncratic risks that can be diversified almost completely in financial markets. Therefore, the risk-neutral probability measure $\mathbb{Q}$ (also known as an associated martingale measure) for the catastrophe-risk variables will coincide with the respective real-world probability measure $\mathbb{P}$. This means that the usual way of pricing the asset using the risk-neutral measure $\mathbb{Q}$, that can be obtained via appropriate change of probability measure, is simply completed using the real-world measure $\mathbb{P}$. Therefore, the stochastic jump processes describing aggregated losses will not change their distributional characteristics as it happens usually when changing from $\mathbb{P}$ to $\mathbb{Q}$ (see, for example, [18, 20] and [15] for a discussion of the above-mentioned approach). To conclude, we use real-world data associated with probability measure $\mathbb{P}$ and due to the Assumption 1 we apply the measure $\mathbb{P}$ further to the pricing.

Let us consider a probability space $(\Omega, \mathcal{F}, \mathbb{P})$ and assume the constant interest rate, then the general pricing formula at time t in the arbitrage-free framework for CAT bonds can be written as (see, e.g., [9]):

$$V_t = e^{-r(T-t)}\mathbb{E}_{\mathbb{P}}\left[P(T)|\mathcal{F}_t\right], \tag{1}$$

where $P(T)$ denotes the payoff at the maturity date T of the bond, $\mathbb{E}_{\mathbb{P}}$ denotes the expectation under the real-world measure, r is the constant interest rate over $[0, T]$ and $\mathcal{F}_t$ is the associated filtration up until time t.

3.1 Single-peril bond pricing

Let us start by defining the basic stochastic process necessary for the construction of CAT bonds. The aggregate loss process (ALP) $L = \{L(t), t > 0\}$ that describes the total amount of losses in time is defined as:

$$L(t) = \sum_{k=1}^{N(t)} X_k, \tag{2}$$

where the process $N = \{N(t), t > 0\}$ is a loss counting process, the loss amounts are positive i.i.d. random variables $\{X_k, k \in \mathbb{N}\}$ with $\mathbb{E}[X_k] = \mu < \infty$. We also assume that N and $\{X_k, k \in \mathbb{N}\}$ are independent.

Given the ALP for a certain risk, the payoff of a ZC CAT bond per unit nominal (a principal amount) with constant recovery rate ρ $(0 \leq \rho \leq 1)$ of the bond, should it be triggered, is given by

$$P_{ZC}(T) = \begin{cases} 1 & \text{if } L(T) < D, \\ \rho & \text{if } L(T) \geq D, \end{cases} \tag{3}$$

where $L(T)$ denotes the aggregate amount of insured losses at T, which is the term of the bond and D is the bond's contractually-specified threshold level triggering the bond.

An arbitrage-free price at the time of issue of the ZC CAT bond with the payoff (3) can be obtained using the formula (1):

$$V_0 = e^{-rT}\mathbb{E}_{\mathbb{P}}\left[\mathbb{I}_{L(T)<D} + \rho\mathbb{I}_{L(T)\geq D}\right] = e^{-rT}\left[\rho + (1-\rho)\mathbb{P}(L(T) < D)\right],$$

where $L(T)$ is the ALP value at T and $\mathbb{I}_A$ denotes the indicator of a given event $A \in \mathcal{F}$.

In the case of a CP CAT bond, having maturity time T, constant coupon rate $c > 0$ and coupon-paying dates $t \in \{t_1, t_2, \ldots, t_k = T\}$ $(k \in \mathbb{N})$, for each coupon paying date $t \in \{t_1, t_2, \ldots, t_k = T\}$, the payoff $P_{CP}(t)$ per unit nominal is:

$$P_{CP}(t) = \begin{cases} c + \mathbb{I}_{\{t=T\}} & \text{if } L(t) < D_{\text{COUPON}}, \\ \rho\left(c + \mathbb{I}_{\{t=T\}}\right) & \text{if } L(t) \geq D_{\text{COUPON}}, \end{cases}$$

where $0 \leq \rho \leq 1$ is the recovery rate defined as in the case of the ZC CAT bond and D_{COUPON} is the predefined threshold level of the CP CAT bond.

Since a CP CAT bond can be considered as a combination of single ZC CAT bonds, its arbitrage-free price at the issue date is:

$$\begin{aligned} V_0 &= \sum_{i=1}^{k} e^{-rt_i}\mathbb{E}_{\mathbb{P}}\left[\left(c + \mathbb{I}_{\{t_i=T\}}\right)\mathbb{I}_{L(t_i)<D_{\text{COUPON}}} + (\rho c + \rho\mathbb{I})\,\mathbb{I}_{L(t_i)\geq D_{\text{COUPON}}}\right] \\ &= \sum_{i=1}^{k} ce^{-rt_i}\left[\rho + (1-\rho)\mathbb{P}(L(t_i) < D_{\text{COUPON}})\right] \\ &\quad + e^{-rT}\left[\rho + (1-\rho)\mathbb{P}(L(T) \geq D_{\text{COUPON}})\right], \end{aligned}$$

where $L(t_i)$ is the ALP value at t_i, D_{COUPON} is the bond's contractually-specified threshold level.

3.2 Multi-peril bond pricing

We construct here a multi-peril CAT bond and propose a pricing methodology for that bond. To this end, we generalise the single-peril approach presented above to the multidimensional case. Let us consider a multidimensional ALP process $\mathbf{L} = (L_1, L_2, \ldots, L_n)$, where $L_i = \{L_i(t), t > 0\}$ denotes the ALP resulting from the i-th peril given by (2) for $i = 1, \ldots, n$.

Firstly, we propose a simple construction of a payoff for a multi-peril zero-coupon (MPZC) CAT bond with a constant recovery rate ρ, $0 \leq \rho \leq 1$. The main idea is that the investor receives the principal of the bond if none of the ALPs L_i exceeded its triggering level D_i $(i = 1, \ldots, n)$ during its term and receives a recovery fraction of the principal if any of the ALPs exceeds its threshold level. Namely, the payoff of the MPZC CAT bond per unit nominal is given by the formula:

$$P_{ZC}^{MP}(T) = \begin{cases} 1 & \text{if } \cap_{i=1}^{n}\{L_i(T) < D_i\} \\ \rho & \text{if } \cup_{i=1}^{n}\{L_i(T) \geq D_i\}, \end{cases} \tag{4}$$

where $D_1, D_2, \ldots, D_n$ are the bond threshold levels for the corresponding ALPs $L_1, L_2, \ldots, L_n$. Here, in Eq. (4), the intersection of events $\cap_{i=1}^{n}\{L_i(T) < D_i\}$ corresponds to the event

that jointly none of the respective ALPs at the maturity $L_1(T), L_2(T), \ldots, L_n(T)$ exceeds respective triggers $D_1, D_2, \ldots, D_n$, while the union of events $\cup_{i=1}^{n}\{L_i(T) < D_i\}$ corresponds to the event that at least one of ALPs at the maturity $L_1(T), L_2(T), \ldots, L_n(T)$ exceeds respective triggers $D_1, D_2, \ldots, D_n$.

By using Assumption 1, the MPZC CAT bond can be priced using the expected value of the payoff under the risk-neutral measure that coincides with the real-world probability measure:

$$V_0 = e^{-rT}\mathbb{E}_{\mathbf{P}}\left[\mathbb{I}_{\cap_{i=1}^{n}\{L_i(T)<D_i\}} + \rho\mathbb{I}_{\cup_{i=1}^{n}\{L_i(T)\geq D_i\}}\right], \tag{5}$$

where $L_1(T), \ldots, L_n(T)$ are the ALP values at T, and $D_1, \ldots, D_n$ are the bond's contractually-specified threshold levels triggering its payoff.

In the case of a multi-peril coupon-paying (MPCP) CAT bond, having maturity time $T > 0$, constant coupon rate $c > 0$ and coupon-paying dates $\{t_1, t_2, \ldots, t_k = T\}$ $(k \in \mathbb{N})$, for each coupon paying date $t \in \{t_1, t_2, \ldots, t_k = T\}$, we introduce the following payoff $P_{CP}^{MP}(t)$ per unit nominal:

$$P_{CP}^{MP}(t) = \begin{cases} c + \mathbb{I}_{\{t=T\}} & \text{if } \cap_{i=1}^{n}\{L_i(t) < D_{i,\text{COUPON}}\}, \\ \rho\left(c + \mathbb{I}_{\{t=T\}}\right) & \text{if } \cup_{i=1}^{n}\{L_i(t) \geq D_{i,\text{COUPON}}\}, \end{cases}$$

where $0 \leq \rho \leq 1$ is defined as in the ZC CAT bond case and $D_{i,\text{COUPON}}$ is the MPCP CAT bond's pre-defined threshold level for i-th peril, and the meaning of events is analogous as in zero-coupon CAT bond, see (4). Similarly, the arbitrage-free price of the bond has the following form:

$$\begin{aligned} V_0 = \sum_{i=1}^{k} e^{-rt_i}\mathbb{E}_{\mathbf{P}}\Big[&\left(c + \mathbb{I}_{\{t_i=T\}}\right)\mathbb{I}_{\cap_{j=1}^{n}\{L_j(t_i)<D_{j,\text{COUPON}}\}} \\ &+\rho\left(c + \mathbb{I}_{\{t_i=T\}}\right)\mathbb{I}_{\cup_{j=1}^{n}\{L_j(t_i)\geq D_{j,\text{COUPON}}\}}\Big], \end{aligned}$$

where $L_j(t_i)$ is the value of $\mathbf{L}$'s j-th marginal process at t_i and $D_{j,\text{COUPON}}$ is the bond's contractually-specified threshold level triggering its payoff for j-th risk.

4 PCS data analysis

In this section, we present a statistical procedure to fit a two-peril CAT bond model introduced in Sect. 3 to natural catastrophe data obtained from PCS. We calibrate and validate two compound non-homogeneous Poisson processes for two distinct perils, namely number of losses related to wind and thunderstorm, and winter storm events. Next, we price a MPZC CAT bond that is triggered if losses caused by at least one of two specified catastrophes exceed given thresholds.

We analyse losses resulting from natural catastrophic events that occurred in the US from 1985 to 2011. Estimates of such losses were provided by PCS. PCS loss index is not an index in the usual financial sense. It is a time series of total insured losses, exceeding USD 25 million, resulting from classified natural catastrophes.

The analysed data set contains information on 807 distinct catastrophes such as wind and thunderstorm events, winter storms, hurricanes, tropical storms, earthquakes, and

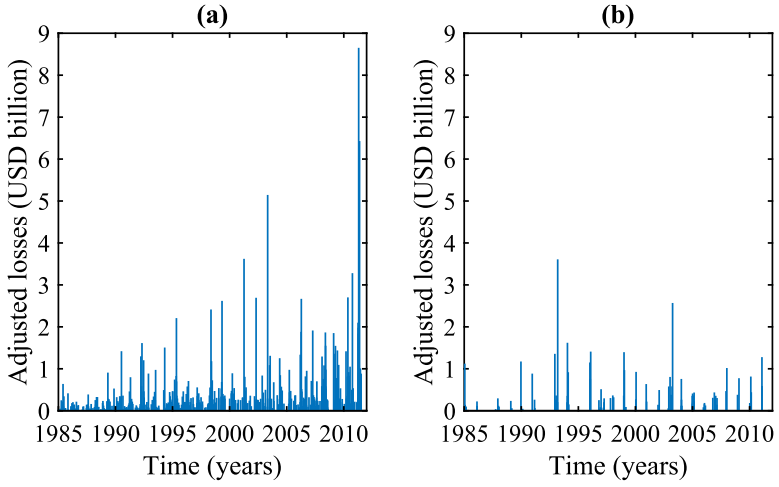

Figure 1 (a) Adjusted losses of wind and thunderstorm, (b) winter storm events

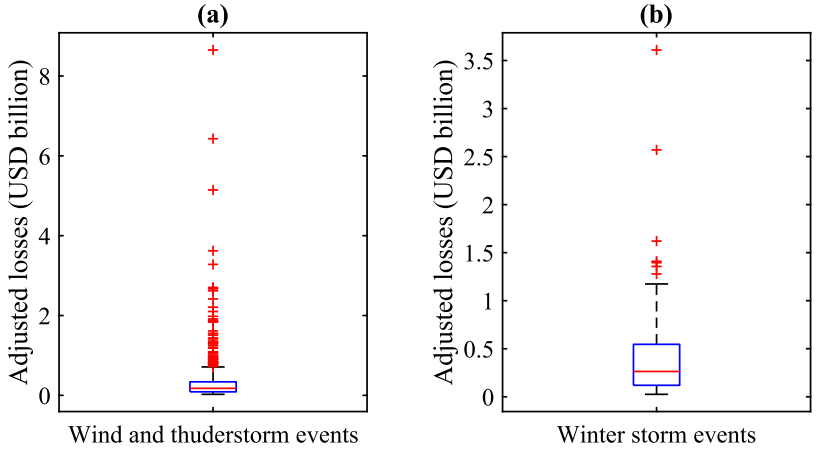

Figure 2 Box plots for adjusted losses of (a) wind and thunderstorm, (b) winter storm events

fires. For our purposes, we chose the two largest subsets of the PCS data set, including 602 cases of wind and thunderstorm losses, see Fig. 1(a), and 96 cases of winter storm losses, see Fig. 1(b). Loss amounts were adjusted using the US customer price index. Basic descriptive statistics of the analysed data sets are presented in Table 1, box plots of the adjusted losses are presented in Fig. 2. For both data sets, we observe positive skewness and the kurtosis values indicate heavy tails of the distributions (for wind and thunderstorm the values are really high).

4.1 Loss amount distributions

The initial stage of the analysis involves fitting a model for the loss amount distribution for wind and thunderstorm events. We must bear in mind that the loss data are left-truncated, as only losses above USD 25 million are reported in the PCS index. Following the statistical procedure described in [25], we fitted six distributions: log-normal, Weibull, Burr, Generalised Pareto (GP), Inverse Gaussian (IG) and Generalised Extreme Value (GEV) by

Table 1 Descriptive statistics of the analysed losses, losses were expressed in USD billion

Peril	Min	Max	Mean	Std	Q1	Q3	Skewness	Kurtosis
Wind and thunderstorm	0.025	8.652	0.348	0.638	0.088	0.338	6.918	70.988
Winter storm	0.026	3.609	0.447	0.542	0.120	0.546	3.061	15.655

Table 2 Loss amount distributions considered to model the PCS losses, defined on the positive reals

Distribution	Density	Constraints
Log-normal	$\frac{1}{x\sigma\sqrt{2\pi}}\exp\left\{\frac{-(\log x-\mu)^2}{2\sigma^2}\right\}$	$\mu\in\mathbb{R},\sigma\geq 0$
Weibull	$\frac{b}{a}\left(\frac{x}{a}\right)^{b-1}\exp\left\{-(\frac{x}{a})^b\right\}$	$a>0,b>0$
Burr	$\frac{kc(\frac{x}{\alpha})^{c-1}}{\alpha(1+(\frac{x}{\alpha})^c)^{k+1}}$	$\alpha>0,c>0,k>0$
GP	$\frac{1}{\sigma}\left(1+\frac{k(x-\theta)}{\sigma}\right)^{-\left(1+\frac{1}{k}\right)}$	$\sigma>0,k\in\mathbb{R},\theta\in\mathbb{R},x>\theta$
IG	$\sqrt{\frac{\lambda}{2\pi x^3}}\exp\left\{-\frac{\lambda}{2\mu^2 x}(x-\mu)^2\right\}$	$\mu>0,\lambda>0$
GEV	$\frac{1}{\sigma}\exp\left\{-\left(1+\frac{k(x-\mu)}{\sigma}\right)^{-\frac{1}{k}}\right\}\times$	$1+\frac{k(x-\mu)}{\sigma}>0,$
	$\left(1+\frac{k(x-\mu)}{\sigma}\right)^{-\left(1+\frac{1}{k}\right)}$	$\sigma>0,k\in\mathbb{R}\backslash\{0\},\mu\in\mathbb{R}$

Table 3 Parameters of fitted distributions and corresponding test statistics for the wind and thunderstorm losses. The *p*-values calculated on the basis of 1000 simulated samples are presented in parentheses

Distribution	Parameters	D	V	W^2	A^2
Log-normal	$\mu=-1.807$,	0.915	1.451	0.746	0.114
	$\sigma=1.142$	*(0.061)*	*(0.050)*	*(0.262)*	*(0.159)*
Weibull	$a=0.180,b=0.629$	1.192	2.178	5.085	0.777
		(0.174)	*(0.012)*	*(0.153)*	*(0.133)*
Burr	$\alpha=0.175,c=1.452,$	0.498	0.964	0.272	0.038
	$k=1.104$	*(0.827)*	*(0.563)*	*(0.857)*	*(0.815)*
GP	$k=0.418,\sigma=0.175,$	0.858	1.574	1.586	0.227
	$\theta=-0.001$	*(0.062)*	*(0.012)*	*(0.045)*	*(0.017)*
IG	$\mu=0.342,\lambda=0.160$	1.289	2.002	1.408	0.248
		(0.000)	*(0.001)*	*(0.009)*	*(0.006)*
GEV	$k=0.594,\sigma=0.117,$	0.494	0.962	0.283	0.041
	$\mu=0.103$	*(0.928)*	*(0.803)*	*(0.946)*	*(0.942)*

the maximum likelihood estimation method. The considered distributions are presented in Table 2 and the parameters of the fitted distribution are given in Table 3.

In Table 3 we can also see the Kolmogorov-Smirnov (D), Kuiper (V), Cramér-von-Mises (W^2), and Anderson and Darling (A^2) test statistic values with the corresponding p-values obtained by Monte Carlo simulations. To this end we closely followed the simulation approach presented in [45]. To calculate the values of the A^2 statistic we used the corrected formulas of [48, 49], which were explicitly presented in [11]. For the truncated case, to account for missing data, the corresponding statistics were computed and the simulations were carried out according to [14].

We can see that the GP and IG distributions are clearly rejected. Of the distributions that are not rejected by the considered statistical tests, the Burr and GEV distributions give the best fit to the considered data.

To confirm our findings, we present in Fig. 3 comparison of the tails of the fitted distributions. We can observe that the Burr and GEV distributions describe the tail behaviour well (surprisingly along with the GP distribution).

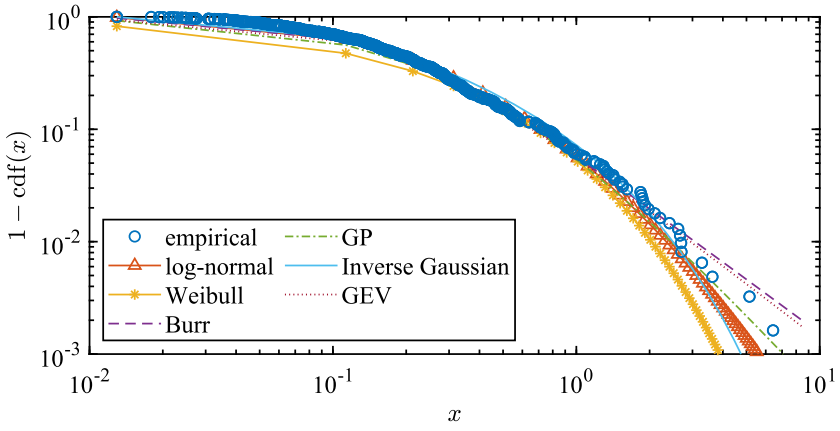

Figure 3 Right tail of the empirical distribution function for the wind and thunderstorm losses, and tails of the fitted distributions in the log-log scale

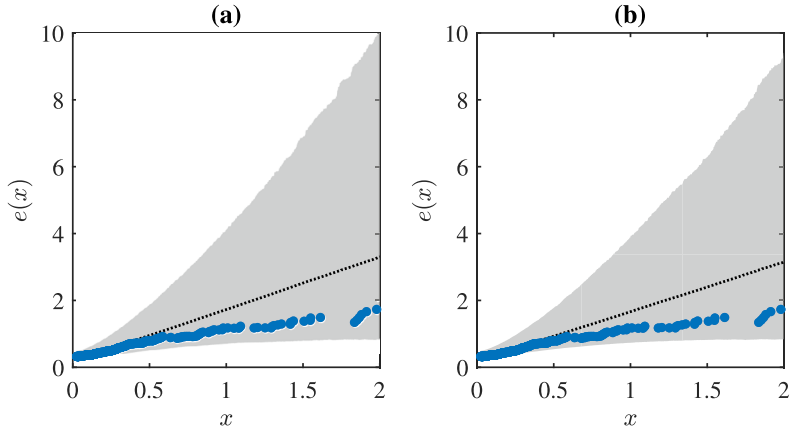

Figure 4 The empirical MEF (blue dots) for the wind and thunderstorm losses compared with MEF's of the fitted distributions (black dotted lines): (a) GEV, (b) Burr. Grey areas represent the 95% confidence intervals corresponding to the fitted distributions

Finally, to confirm the usefulness of the fit, we analyse the mean excess function (MEF). The MEF $e(x)$ is the expected payment per loss X on a policy with a fixed amount deductible of x, where losses with amounts less than or equal to x are completely ignored:

$$e(x) = \mathrm{E}(X - x | X > x). \tag{6}$$

The empirical counterpart $\hat{e}_n$ based on a representative sample $x_1, \ldots, x_n$ is defined as:

$$\hat{e}_n(x) = \frac{\sum_{x_i > x} x_i}{\#\{i : x_i > x\}} - x. \tag{7}$$

If the loss amount distribution is heavier-tailed than the exponential, the MEF ultimately increases, and when it is lighter-tailed, the MEF ultimately decreases. Hence, the shape of $e(x)$ or its empirical counterpart provides important information on the sub-exponential

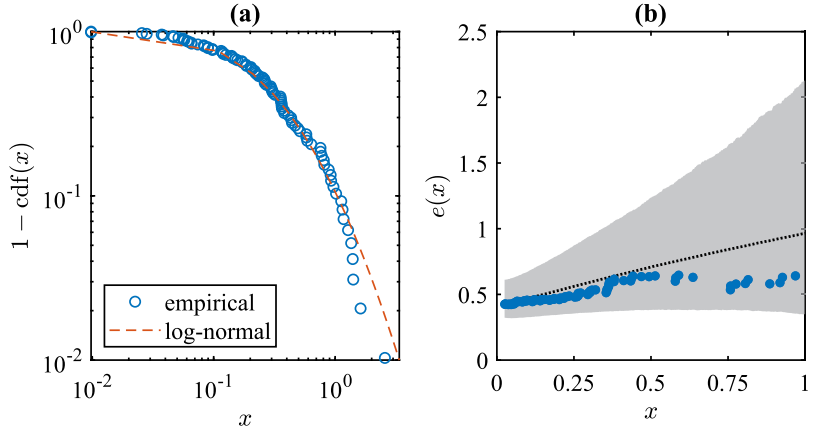

Figure 5 (a) Right tail of the empirical distribution function for the winter storm losses and of the fitted log-normal distribution in the log-log scale. (b) The empirical MEF (blue dots) for the winter storm losses compared with the MEF of the fitted log-normal distribution (dotted black line) presented with the grey area describing the fitted distribution 95% confidence interval

or super-exponential nature of the tail (for more information about the MEF and its properties, we refer to [11]).

In Fig. 4 we can see the comparison of the empirical MEF with the MEFs corresponding to the two best-fitted distributions. The latter was obtained by Monte Carlo simulations. We also added 95% confidence regions for MEFs of the fitted distributions (calculated on the basis of 10K simulated samples of the same size as the original data) to see if the empirical MEF is included in that region. First, we can clearly see that the empirical function is a strictly increasing function, which is common to the heavy-tailed distributions. Second, in both cases, the sample MEF fits within the interval.

The second data set is significantly smaller than the first one, as it contains only 96 observations about winter storm-related losses. Thus, we propose a quite flexible distribution, with only two parameters, often used in the modelling of heavy-tailed insurance losses, namely the log-normal distribution. The fitted parameters $\mu = -1.410$ and $\sigma = 1.129$. Similarly, as before, we checked the goodness-of-fit by performing the statistical tests. The p values of the Kolmogorov-Smirnov, Kuiper, Cramér-von-Mises and Anderson and Darling test were equal to 0.909, 0.825, 0.795 and 0.744, respectively. This indicates that the log-normal distribution gives a good fit to our data.

We also compared the right tail of the empirical and fitted distribution functions, see Fig. 5 (a). Finally, in Fig. 5(b), we also compare the sample MEF with the MEF of the fitted distribution and the corresponding confidence interval. We can observe that the empirical MEF fits the region well, which confirms the goodness-of-fit.

4.2 Intensity functions

The second part of the modelling is related to finding an appropriate counting process that will describe the moments when natural catastrophes occur, see formula (2). For that purpose, we choose the non-homogeneous Poisson process $N(t)$ with a non-negative, deterministic, time-varying intensity $\lambda(t)$.

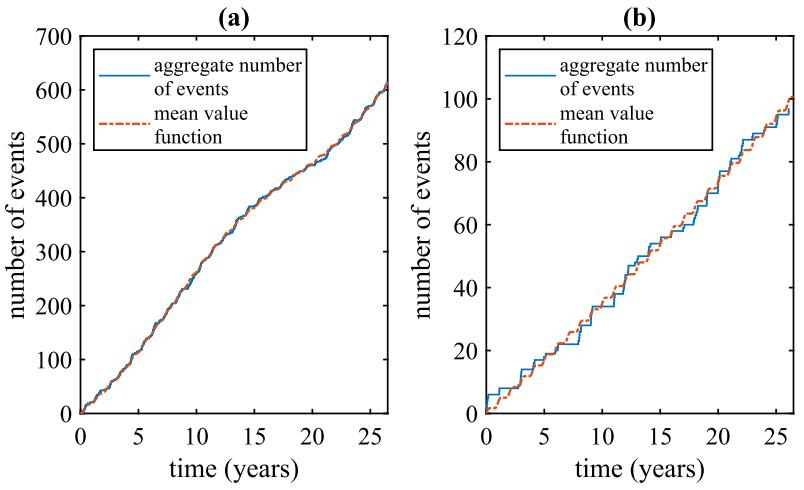

Figure 6 (a) The aggregate number of wind and thunderstorm, (b) winter storm events, and mean value functions corresponding to the fitted intensity functions

An intensity function based on sine functions allows us to capture the apparent seasonality of considered wind and thunderstorm events:

$$\lambda_1(t) = a_1 + b_1 \sin(2\pi(t + c_1)) + d_1 \sin\left(\frac{2\pi}{\omega}(t + e_1)\right), \tag{8}$$

where a_1 describes the average number of events per year, the first sine function with amplitude b_1, shift of c_1 years and period of one year captures the yearly fluctuations in the number of events and the second sine function with amplitude d_1, shift of e_1 years and period of ω years describers the long-term seasonality. The parameters of the intensity function $\lambda(t)$ were fitted using the least-squares method by comparing the mean value function $\mathbb{E}N(t) = \int_0^t \lambda(s)\,ds$ with the aggregate number of losses. We obtained the following parameters of the intensity function: $a_1 = 22.89$, $b_1 = 15.26$, $c_1 = -6.09$, $d_1 = 7.53$, $e_1 = -2.62$ and $\omega = 20.76$. The mean-squared error (MSE) is equal to 10.1851, the mean absolute error (MAE) is 2.5193 and mean average percentage error (MAPE) is equal to 1.96%. The fitted intensity function is illustrated in Fig. 6(a). We can see that the mean value function fits the aggregate number of losses quite well. Finally, we note that we also considered other combinations of polynomial and sine functions but they did not lead to better results.

While winds and thunderstorms strike the country throughout the year, winter storms occur only from October to April, with the majority occurring between December and February. Knowing that the intensity of events should be equal to zero for almost half of the year, we propose the following intensity function to describe the winter storm occurrences:

$$\lambda_2(t) = \max\{a_2 + b_2 t + c_2 \cos(2\pi x); 0\}. \tag{9}$$

The parameters fitted to the PCS data are $a_2 = -1.08$, $b_2 = 12.08$ and $c_2 = 0.07$. The MSE is equal to 4.6947, MAE equal to 1.8848 and MAPE equal to 10.21%. The mean value function corresponding to the fitted intensity function is presented in Fig. 6(b) and the fit result is quite acceptable.

4.3 Illustration of the prices of a two-peril ZC CAT bond

To illustrate the dynamics of the prices of MPZC CAT bonds we consider two perils that were studied before: wind and thunderstorm, and winter storm events. We assume that the bond is triggered if one of the aggregate loss processes exceeds a specified threshold.

For simplicity, we assume the recovery rate $\rho = 0$. Since the two considered perils appear independent, the arbitrage-free pricing formula presented in Sect. 3.2 reduces to:

$$V_0 = e^{-rT}\mathbb{E}_{\mathbb{P}}\left[\mathbb{I}_{\{L_1(T)<D_1\}\cap\{L_2(T)<D_2\}}\right] = e^{-rT}\mathbb{E}_{\mathbb{P}}\left[\mathbb{I}_{\{L_1(T)<D_1\}}\mathbb{I}_{\{L_2(T)<D_2\}}\right]$$
$$= e^{-rT}\mathbb{P}(L_1(T) < D_1)\mathbb{P}(L_2(T) < D_2),$$

where L_1 and L_2 are ALPs corresponding to wind and thunderstorm events and winter storm events, respectively. Moreover, as we use non-homogeneous Poisson processes for modelling the occurrence of the losses, we can also express the probabilities of not exceeding thresholds D_1 and D_2 by L_1 and L_2 in the following way

$$\mathbb{P}\left(L_i(T) < D_i\right) = \sum_{n=0}^{\infty} e^{-\int_0^T \lambda_i(u)\mathrm{d}u} \frac{\left(\int_0^T \lambda_i(u)\mathrm{d}u\right)^n}{n!} F_{X_i}^{n*}(D_i),$$

where F_{X_i} denotes the cumulative density function of the losses caused by i-th risk and $F_{X_i}^{n*}$ denotes the n-fold convolution of F_{X_i} with itself, for $i = 1, 2$.

We assume that $r = 3\%$ and the maturity time of the bond is $T = 2$ years. The threshold D_1 for wind and thunderstorm losses changes from 25 to 40 USD billion, while the threshold D_2 for winter storm losses varies from 6 to 10 billion USD. We calculate the prices on the basis of the 20 000 Monte Carlo simulations and present the results in Fig. 7, separately for the Burr and GEV distributions, as they were best fitted for wind and thunderstorm losses. We can see that the two-peril ZC CAT bond prices clearly decrease as the threshold levels D_1 or D_2 drop and the prices obtained with the use of the Burr distribution are lower than those obtained with the GEV. Based on the results depicted in Fig. 7 one can propose a fair price of two-peril ZC CAT bonds related to wind and thunderstorm losses, and winter storm losses for respective threshold levels. The choice of a lower threshold level value D_1 (or/and D_2) leads to a lower price of the two-peril ZC CAT bond, but is associated with a higher chance and higher risk of exceeding the threshold by the associated ALP and therefore loosing a $1 - \rho$ of the principal by the investor. On the other hand, by increasing the parameter D_1 (or/and D_2) of the two-peril ZC CAT bond lead to a higher price of the bond, which is associated with lower chances of loosing the principal by the investor. In Fig. 8 we can also see the differences between the Burr and GEV prices for wide ranges of D_1 and D_2. We can observe that the absolute maximum difference in the investigated region reaches 0.006 per 100 of the principal. Therefore, the choice between the two respective distributions of underlying losses for wind and thunderstorm losses results in very small differences in prices.

5 Conclusions

Insurers typically deal with natural catastrophe risk by either transferring it to the reinsurance market or securitising this risk in the capital markets. Until fairly recently, property reinsurance was a relatively well-understood market with efficient pricing. We also note

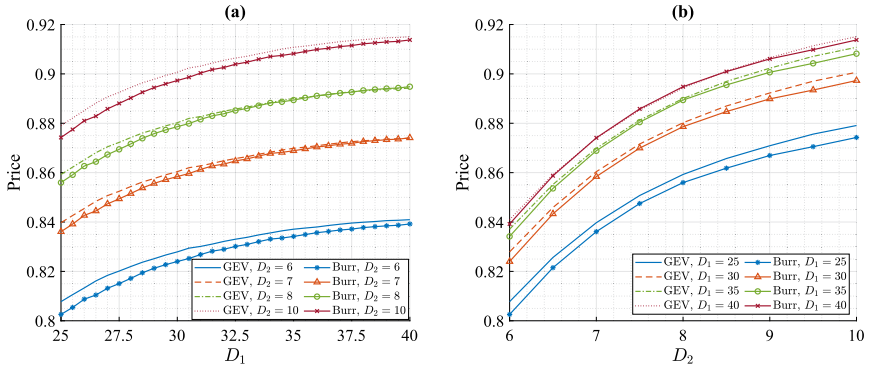

Figure 7 Two-peril ZC CAT bond prices with GEV (lines without markers) and Burr (lines with markers) distributions used for wind and thunderstorm losses with (a) fixed D_2, with respect to D_1, and (b) fixed D_1, with respect to D_2

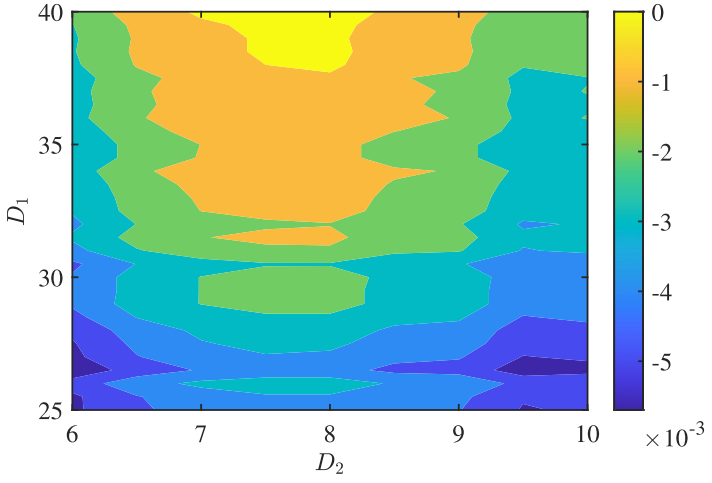

Figure 8 Contour plot of differences between the two-peril ZC CAT bond prices obtained with the use of the Burr and GEV distributions

structured reinsurance deals whose indemnification scheme is contingent upon the performance of the insurer buying it, for instance measured in terms of his loss ratio relative to the average loss ratio of the market [54], or optimal risk sharing arrangements with multiple risk environments [2].

However, natural disasters, such as earthquakes and hurricanes, are increasingly exerting a dominant impact on the industry. In part, this is due to the rapidly changing heterogeneous distribution of high-value property in vulnerable areas. A consequence of this has been an increased need for a primary and secondary market in catastrophe-related insurance derivatives.

Since capital markets have access to larger, more diversified and more liquid pools of capital, as opposed to the equity of reinsurers, such capital markets possess a notable advantage over reinsurance markets when it comes to financing catastrophe risk [22]. The search for ways of accessing alternative, rich and robust sources of capital has led to a wave of innovative financial products.

The relative attractiveness of ILS, especially to large pension funds, compared to traded equity and corporate debt, stems from the fact that they are less correlated with the financial markets and often attract higher yields compared to traded corporate debt. For governments, having a source of disaster risk financing and insurance provided by catastrophe bonds can help the government borrow more on the capital markets, improve its standing with debtors and ultimately provide welfare gains to the population [6].

Adequate pricing of ILS instruments can help to better inform pricing decisions for insurance and reinsurance companies, structuring banks, dealers and institutional investors at issue. In this paper, we focused on CAT bonds being a prominent example of ILS [17]. Although most CAT bonds rely on a single trigger, in some cases multiple triggers are used. CAT bonds can be separated into several tranches that vary in terms of the trigger, reference peril, and covered territory. Thus, we strongly believe that there is a need for the development of multi-region and multi-peril ILS pricing techniques.

In this paper, we addressed the issue of modelling and pricing of multi-peril CAT bonds which are triggered if the losses corresponding to one of the perils exceed a certain threshold specific to the peril. We constructed ZC and CP multi-peril CAT bonds and presented their arbitrage-free prices. We also performed a fitting and validation procedure for the US natural catastrophe data from the years 1985-2011 provided by PCS taking into account the fact that the data are left-truncated. For the analysis we selected two perils, namely wind and thunderstorm, and winter storm events. We believe that the procedure is quite universal and can be applied to various catastrophe data.

We considered the case when two perils are independent. We would like to emphasise that the price of the multi-peril bond for the independent case is much lower than the sum of prices for two separate bonds. As explained in [34], the coverage for an either/or event with a binary payout is the functional equivalent of covering the first event of the two covered perils. Then the issuer is left with a residual exposure of the second event. Hence, the issuer will suffer a retained loss if there is loss for both perils.

As a result, we obtained a two-dimensional model with two aggregate non-homogeneous Poisson processes describing the flow of losses. The model was validated with the use of visual tools and rigorous statistical tests that confirmed that Burr and GEV distributions are appropriate for the wind and thunderstorm losses and log-normal distribution for the winter storm losses.

Finally, we illustrated the two-peril ZC CAT bonds prices with the use of Monte Carlo simulations for the best-fitted models by assuming the zero recovery rate and by considering different threshold levels for the two perils. We addressed the pricing of multi-peril ILS tied to industry loss indices or actual losses of an insurer. The work can be further generalised to multi-peril and multi-region ILS also taking into account the data where the driving loss processes exhibit dependence.

Author contributions

KB and MT: conceptualization; KB, MT, MZ: methodology; MZ: software; MZ: formal analysis and investigation; MZ: writing—original draft preparation; KB, MT, MZ: writing—review and editing; KB, MT: supervision. All authors read and approved the final manuscript.

Funding

This work was supported by the NCN Opus 24 Grant No. 2022/47/B/HS4/02139.

Data availability

The datasets used and/or analysed during the current study are available from the corresponding author on reasonable request.

Declarations

Competing interests
The authors declare that they have no competing interests.

Received: 1 December 2023 Accepted: 19 July 2024 Published online: 31 July 2024

References

1. Artemis. Catastrophe bond and insurance-linked securities deal directory. 2022. http://www.artemis.bm/deal-directory/.
2. Asimit AV, Boonen TJ, Chi Y, Chong WF. Risk sharing with multiple indemnity environments. Eur J Oper Res. 2021;295(2):587–603. https://doi.org/10.1016/j.ejor.2021.03.012. https://www.sciencedirect.com/science/article/pii/S0377221721002022.
3. Bakshi G, Madan D. Average rate claims with emphasis on catastrophe loss options. J Financ Quant Anal. 2002;37(1):93–115.
4. Beer S, Braun A. Market-consistent valuation of natural catastrophe risk. J Bank Finance. 2022;134:106350. https://doi.org/10.1016/j.jbankfin.2021.106350.
5. Blöschl G, Hall J, Viglione A et al. Changing climate both increases and decreases European river floods. Nature. 2019;573:108–11.
6. Borensztein E, Cavallo E, Jeanne O. The welfare gains from macro-insurance against natural disasters. J Dev Econ. 2017;124:142–56. https://doi.org/10.1016/j.jdeveco.2016.08.004.
7. Braun A. Pricing catastrophe swaps: a contingent claims approach. Insur Math Econ. 2011;49(3):520–36.
8. Braun A. Pricing in the primary market for CAT bonds: new empirical evidence. J Risk Insur. 2016;83(4):811–47.
9. Burnecki K, Giuricich MN. Stable weak approximation at work in index-linked catastrophe bond pricing. Risks. 2017;5(4). https://doi.org/10.3390/risks5040064.
10. Burnecki K, Giuricich MN, Palmowski Z. Valuation of contingent convertible catastrophe bonds – the case for equity conversion. Insur Math Econ. 2019;88:238. https://doi.org/10.1016/j.insmatheco.2019.07.006.
11. Burnecki K, Janczura J, Weron R. Building loss models. 2nd ed. In: Čížek P, Härdle W, Weron R, editors. Statistical tools for finance and insurance. Berlin: Springer; 2011. p. 293–328.
12. Burnecki K, Kukla G. Pricing of zero-coupon and coupon CAT bonds. Appl Math. 2003;30(3):315–24.
13. Chang CW, Chang JS. An integrated approach to pricing catastrophe reinsurance. Risks. 2017;5(3):51.
14. Chernobai A, Burnecki K, Rachev S, Trück S, Weron R. Modelling catastrophe claims with left-truncated severity distributions. Comput Stat. 2006;21(3–4):537–55.
15. Cox SH, Pedersen HW. Catastrophe risk bonds. N Am Actuar J. 2000;4(4):56–82.
16. Cox SH, Schwebach RG. Insurance futures and hedging insurance price risk. J Risk Insur. 1992;59(4):628–44.
17. Cummins JD. CAT bonds and other risk-linked securities: state of the market and recent developments. Risk Manag Insur Rev. 2008;11(1):23–47.
18. Cummins JD, Geman H. Pricing catastrophe insurance futures and call spreads: an arbitrage approach. J Fixed Income. 1995;4(4):46–57.
19. Cummins JD, Weiss MA. Convergence of insurance and financial markets: hybrid and securitized risk-transfer solutions. J Risk Insur. 2009;76(3):493–545.
20. Delbaen F, Haezendonck J. A martingale approach to premium calculation principles in an arbitrage free market. Insur Math Econ. 1989;8(4):269–77.
21. Doherty NA. Innovations in managing catastrophe risk. J Risk Insur. 1997;64(4):713–8.
22. Durbin D. Managing natural catastrophe risks: the structure and dynamics of reinsurance. Geneva Pap Risk Insur, Issues Pract. 2001;26:297–309.
23. Froot KA. The market for catastrophe risk: a clinical examination. J Financ Econ. 2001;60(2):529–71.
24. Gatzert N, Pokutta S, Vogl N. Convergence of Capital and Insurance Markets: Consistent Pricing of Index-Linked Catastrophic Loss Instruments. 2014. Tech. Rep.
25. Giuricich M, Burnecki K. Modelling of left-truncated heavy-tailed data with application to catastrophe bond pricing. Phys A, Stat Mech Appl. 2019;525:498–513.
26. Götze T, Gürtler M, Witowski E. Improving cat bond pricing models via machine learning. J Asset Manag. 2020;21:428–46. https://doi.org/10.1057/s41260-020-00167-0.
27. Härdle WK, Cabrera BL. Calibrating CAT bonds for Mexican earthquakes. J Risk Insur. 2010;77(3):625–50. https://doi.org/10.1111/j.1539-6975.2010.01355.x.
28. Haslip GG, Kaishev VK. Pricing of reinsurance contracts in the presence of catastrophe bonds. ASTIN Bull. 2010;40(01):307–29.
29. Hofer L, Zanini MA, Gardoni P. Risk-based catastrophe bond design for a spatially distributed portfolio. Struct Saf. 2020;83:101908. https://doi.org/10.1016/j.strusafe.2019.101908.
30. Jaimungal S, Wang T. Catastrophe options with stochastic interest rates and compound Poisson losses. Insur Math Econ. 2006;38(3):469–83.
31. Lane M. Regressions and machine learning - some observations, some lessons. Lane Financial LLC. 2018.
32. Lane M, Beckwith R. The loss file - natural catastrophe ILS issues 2001-2020. Lane Financial LLC; 2021.
33. Lane MN. Pricing risk transfer transactions. ASTIN Bull. 2000;30(2):259–93.
34. Lane MN. Arbitrage algebra and the price of multi-peril ILS. J Risk Finance. 2004;5(2):45–51.
35. Lee JP, Yu MT. Pricing default-risky CAT bonds with moral hazard and basis risk. J Risk Insur. 2002;69(1):25–44.
36. Lee JP, Yu MT. Valuation of catastrophe reinsurance with catastrophe bonds. Insur Math Econ. 2007;41(2):264–78.
37. Ma ZG, Ma CQ. Pricing catastrophe risk bonds: a mixed approximation method. Insur Math Econ. 2013;52(2):243–54.
38. Major JA. Methodological considerations in the statistical modeling of catastrophe bond prices. Risk Manag Insur Rev. 2019;22(1):39–56. https://doi.org/10.1111/rmir.12114.
39. Merton RC. Option pricing when underlying stock returns are discontinuous. J Financ Econ. 1976;3(1):125–44.
40. Ni W, Henshaw K, Zhu W, Wang J, Hu M, Constantinescu C. On flood risk management across socioeconomic environments. An Inst Actuar Esp. 2020;26:71–122. https://doi.org/10.26360/2020_4.

41. Nowak P, Romaniuk M. Pricing and simulations of catastrophe bonds. Insur Math Econ. 2013;52(1):18–28. https://doi.org/10.1016/j.insmatheco.2012.10.006.
42. Nowak P, Romaniuk M. Valuing catastrophe bonds involving correlation and CIR interest rate model. Comput Appl Math. 2018;37:365–94. https://doi.org/10.1007/s40314-016-0348-2.
43. Petracou EV, Xepapadeas A, Yannacopoulos AN. Decision making under model uncertainty: Fréchet–Wasserstein mean preferences. Manag Sci. 2021;68:1195–211. https://doi.org/10.1287/mnsc.2021.3961.
44. Reshetar G. Pricing of multiple-event coupon paying CAT bond. 2008. Available at SSRN. https://doi.org/10.2139/ssrn.1059021.
45. Ross S. Simulation. San Diego: Academic Press; 2002.
46. Salustro C. Severe Convective Storm Modelling. Presented to the CAS (2013). www.casact.org/community/affiliates/canw/0913/Salustro.pdf.
47. Shao J, Pantelous A, Papaioannou AD. Catastrophe risk bonds with applications to earthquakes. Eur Actuar J. 2015;5:113–38. https://doi.org/10.1007/s13385-015-0104-9.
48. Stephens MA. EDF statistics for goodness of fit and some comparisons. J Am Stat Assoc. 1974;69(347):730–7.
49. Stephens MS. Tests based on EDF statistics. In: D'Agostino RB, Stephens MS, editors. Goodness-of-fit techniques. New York: Dekker; 1986.
50. SwissRe: sigma 2/2020: Natural catastrophes in times of economic accumulation and climate change. Zurich, Switzerland. 2020.
51. SwissRe: sigma 1/2021: Natural catastrophes in 2021: the floodgates are open. Zurich, Switzerland. 2022.
52. Tang Y, Wen C, Ling C, Zhang Y. Pricing multi-event-triggered catastrophe bonds based on a copula-POT model. Risks. 2023;11(8). https://doi.org/10.3390/risks11080151. https://www.mdpi.com/2227-9091/11/8/151.
53. Vaugirard VE. Pricing catastrophe bonds by an arbitrage approach. Q Rev Econ Finance. 2003;43(1):119–32.
54. Vincent L, Albrecher H, Krvavych Y. Structured reinsurance deals with reference to relative market performance. Insur Math Econ. 2021;101:125–39. https://doi.org/10.1016/j.insmatheco.2021.07.006. https://www.sciencedirect.com/science/article/pii/S0167668721001189.
55. Zimbidis AA, Frangos NE, Pantelous AA. Modeling earthquake risk via extreme value theory and pricing the respective catastrophe bonds. ASTIN Bull. 2007;37(1):163–83.

Publisher's Note